J. Appl. Comput. Mech., 8(4) (2022) 1236-1245
DOI: 10.22055/JACM.2021.35353.2638

ISSN: 2383-4536
jacm.scu.ac.ir

Shahid Chamran
University of Ahvaz

Journal of
Applied and Computational Mechanics

Research Paper

Theoretical Investigation of Viscosity and Thermal Conductivity of a Gas along a Non-isothermal Vertical Surface in Porous Environment with Dissipative Heat: Numerical Technique

Silpi Hazarika[1], Sahin Ahmed[2]

[1] Department of Mathematics, Rajiv Gandhi University, Arunachal Pradesh, India, 791112 Email: silpi.hazarika@rgu.ac.in

[2] Department of Mathematics, Rajiv Gandhi University, Arunachal Pradesh, India, 791112 Email: sahin.ahmed@rgu.ac.in

Received October 09 2020; Revised February 16 2021; Accepted for publication March 03 2021.
Corresponding author: S. Ahmed (sahin.ahmed@rgu.ac.in)

Abstract. The prime objective of the current investigation is to explore the variation of viscosity and thermal conductivity impacts on MHD convective flow over a moving non-isothermal vertical plate in presence of the viscous-dissipative heat and thermal-radiation. The compatible transformation of similarity are employed to obtain the non-linear ODE with the appropriate boundary conditions from the governing equations and the numerical solution of the boundary value problem so obtained are solved via MATLAB bvp4c solver. Naturally, the fluid viscosity and thermal-conductivity may vary from liquid to metal with temperatures and therefore, the impact of viscosity and thermal-conductivity in this investigation is quite significant. The physical parameters along with several influences on momentum, temperature, and concentration are explicated and portrayed with graphs. In addition, the velocity, temperature and concentration gradients at the surface are evaluated and displayed in tabular form. A decent agreement is found in the present outcomes with previously issued work. Furthermore, it is found that the growth of the thermal-radiation increases the gas temperature. The present study is useful for various industrial applications like metal and polymer extrusion, continuous casting, cooling process, nuclear plant and many more.

Keywords: Dissipative heat, Fluid Viscosity and Thermal Conductivity, Soret effect, Thermal radiation, magnetic drag force method.

1. Introduction

In nature, viscosity and thermal conductivity may vary with the variation of temperature and experimentally they have important applications in different branches of manufacturing industries such as metal and polymer extrusion, drawing of plastic sheets, Optimizing and assessing dispersion stability, Viscoelastic fingerprinting of materials to determine the extent of solid-like or liquid-like behavior. The law of viscosity has important uses in such areas as inkjet printing, protein formulations and injections, and even food and beverage manufacturing.

The hydromagnetic flow in electrically conducting fluid is necessarily play an important role in the fields like- agriculture, engineering, petroleum industry and can control the rate of cooling and the desired quality of product can be achieved [1, 25]. Also in the presence of magnetic field, the convection heat transfer is very useful in astrophysics and geophysics. Sakiadis [2] was the first researcher who has developed a numerical solution using similarity transformations for a steady flow over a surface. Some pioneer works on MHD heat transport have incorporated here. Heat transfer along an isothermal vertical plate with natural convection had investigated by Cheesewright [3]. Two-dimensional laminar natural convection flow due to unsteadiness of viscous fluid over an infinite plane vertical surface in a porous medium was examined by Helmy [4]. Molla *et al.* [5] investigated the waviness of surfaces on free convection heat transport. Soundalgekar *et al.* [6] had presented the behaviour of constant suction and heat source for unsteady natural convection flow. Steady-state solutions of unsteady MHD free convective heat and mass transfer flow for Soret effect on induced magnetic field and thermal diffusion investigated by Zueco et al. [7] and Ahmed et al. [8] studied 3D flow with twin effects of magnetic field and heat flux.

The physical properties of the ambient fluid had considered constants in the above-mentioned citations by the authors. It is worth mentioning that the physical properties of fluid like viscosity [9 – 13] may change with temperature significantly. Within the momentum boundary layer, transport phenomena may be raising by suppressing the fluid viscosity when the fluid temperature increases and therefore, more effect of rate of heat transfer will occurred at the wall. In such situations, it is necessarily to consider the effect of viscosity of the fluid, which depends on temperature for the present investigation. On the effects of variable viscosity and thermal conductivity, some investigators like Salem [14], Chiam [15], Pantokratoras [16] and Mukhopadhyay and Layek [17] have devoted their research in viscous fluids over surfaces with various constrains and they discussed the necessity of variable viscosity significantly.

Published online: April 01 2021

Mahanti *et al.* [18] presented the steady natural convection flow for the variation of viscosity and thermal-conductivity. Researchers [19, 21] have studied the thermal-conductivity of liquids with MHD heat transport due to low Prandtl number. The effect of viscosity and thermal-diffusivity on mixed convection flow over a stretching sheet was discussed Seddeek and Salem [20]. The similarity solution of MHD natural convection on an inclined plate with internal heat generation / absorption has obtained Chamkha and Khaled [22]. Convective MHD heat and mass transfer flow along a moving non-isothermal vertical surface in association with heat generation has analyzed by Subhakar *et al.* [23]. Micropolar fluid in a vertical cone with the effect of variable viscosity and thermal conductivity has analyzed Hazarika *et al.* [24]. Numerous latest studies have been done on heat transport for the use of different fluid and physical factors in recent years [26-36]. Hazarika *et al.* [38] has investigated the behaviour of hydromagnetic heat transport of Cu-water nanofluids due to the application of diffusion-thermo in porous regime by infinite series solution and they explained that the velocity of Cu-nanoparticles are higher in comparison to water base fluid by the impact of free convection and diffusion-thermo. Hazarika and Ahmed [39] have analyzed the behavior of MHD free convective flow of Casson-fluid in a vertical channel of porous structures covered by Carbon Nano-tubes, where thermal radiation and heat generation assume a significant role in CNT's. Ahmed *et al.* [37] have developed a numerical solution through bvp4c for the impact of viscosity and thermal conductivity of heat transport in hydromagnetic fluid over a non-isothermal vertical surface and the importance of such analysis is found in metal and polymer extrusion.

In view of the above analysis, it is worth mentioning that the physical properties like viscosity and thermal conductivity always vary with temperature in boundary layer. In the above cited analysis, it is observed that most of the studies are depends on variation of viscosity and thermal conductivity. In this investigation, the fluid is supposed to have variable viscosity and thermal-conductivity by means of an inverse linear function of temperature. Therefore, the main objectives of this study is that to examine the major effects of variation of viscosity and thermal conductivity on steady MHD convection radiating flow over an stretched sheet with Soret and Dufor effects. Impact of low and high radiation along with free convection due to mass transfer and viscous dissipation are also included. By similarity transformations, the highly coupled non-linear PDE's are converted to a set of high order ODE's and then solved numerically by employing MATLAB bvp4c solver method.

2. Mathematical Formulation

In this investigation, we have presented a flow model in Fig. 1, for a steady state laminar convective flow along a non-isothermal and non-conducting vertical plate moving with a uniform velocity U_0 in a saturated porous medium. Here the fluid is viscous, electrically conducting, incompressible and H_0 is the intensity of magnetic field normal to the surface. The coordinate system is considered as the ζ -axis is taken along the surface and ξ -axis is normal to the surface oriented into the fluid medium. At the surface, $\xi = 0$, the temperature of fluid is $\overline{T}_w$ and away the surface it is $\overline{T}_\infty$. At $\zeta = 0$, the fluid temperature is $\overline{T}_0$. Also temperature of the fluid is $\overline{T}$. As the magnetic field is not very strong in this study, therefore, the external electric field for charge polarization and Hall effects become vanishes.

Therefore, the boundary layer equations of the proposed model in connection with the variation of fluid viscosity and thermal-conductivity are [11, 15, 25]

$$\overline{U}_\zeta + \overline{V}_\xi = 0\,, \tag{1}$$

$$\overline{U}\overline{U}_\zeta + \overline{V}\overline{U}_\xi = \left(\nu \overline{U}_\xi\right)_\xi + g\beta_T\left(\overline{T} - \overline{T}_\infty\right) + g\beta_C\left(\overline{C} - \overline{C}_\infty\right) - \left(\frac{\nu}{\overline{K}_P} + \frac{\sigma H_0^2}{\rho}\right)\overline{U}\,, \tag{2}$$

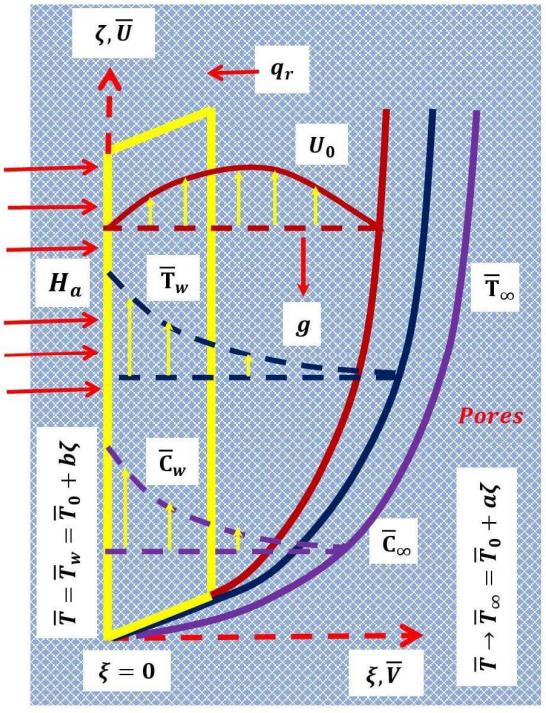

Fig. 1. Flow Model and Coordinate System.

$$\rho C_P\left(\overline{U}\overline{T}_\zeta+\overline{V}\overline{T}_\xi\right)=\left(\lambda\overline{T}_\xi\right)_\xi+\frac{\rho D_m K_T}{C_S}\overline{C}_{\xi\xi}+Q_0\left(\overline{T}-\overline{T}_\infty\right)+\mu\left(\overline{U}_\xi\right)^2+\left(q_r\right)_\xi, \tag{3}$$

$$\overline{U}\overline{C}_\zeta+\overline{V}\overline{C}_\xi=D_m\overline{C}_{\xi\xi}+\frac{D_m K_T}{T_m}\overline{T}_{\xi\xi}, \tag{4}$$

where $(\ )_\zeta$ and $(\ )_\xi$ stand for partial differentiations w. r. t. ζ and ξ, respectively. The fluid viscosity [11] is given by

$$\mu^{-1}=\mu_\infty^{-1}\left[1+\delta\left(\overline{T}-\overline{T}_\infty\right)\right], \tag{5}$$

or

$$\mu^{-1}=a\left(\overline{T}-\overline{T}_c\right), \text{ where } a=\delta\mu_\infty^{-1} \text{ and } \overline{T}_c=\overline{T}_\infty-\delta^{-1}.$$

The thermal conductivity [11] is defined as

$$\lambda^{-1}=\lambda_\infty^{-1}\left[1+\xi\left(\overline{T}-\overline{T}_\infty\right)\right], \tag{6}$$

or

$$\lambda^{-1}=b\left(\overline{T}-\overline{T}_r\right), \text{ where } b=\delta\xi\lambda_\infty^{-1} \text{ and } \overline{T}_r=\overline{T}_\infty-\xi^{-1}.$$

The radiative heat flux [38, 39] is given by,

$$\left(q_r\right)_\xi=-4\alpha^2\left(\overline{T}-\overline{T}_\infty\right), \text{ where } \overline{T}^4\cong 4\overline{T}_\infty^3-3\overline{T}_\infty^4 \tag{7}$$

The equations are subjected to the following boundary conditions

$$\left.\begin{aligned}&\overline{U}=U_0,\ \overline{V}=0,\ \overline{T}=\overline{T}_w=\overline{T}_0+b\zeta,\ \overline{C}=\overline{C}_w \text{ at } \xi=0\\&\overline{U}\to 0,\ \overline{T}=\overline{T}_\infty=\overline{T}_0+a\zeta,\ \overline{C}\to\overline{C}_w \text{ as } \xi\to 0\end{aligned}\right\} \tag{8}$$

The equation of continuity (1) is satisfied identically by the Cauchy-Riemann equations

$$\overline{U}=\psi_\xi,\ \overline{V}=-\psi_\zeta, \tag{9}$$

where $\psi(\zeta,\xi)$ is the stream-function. Let us introduce the following non-dimensional quantities and similarity variables

$$\left.\begin{aligned}&H_a=\frac{\sigma H_0^2\zeta^2}{\mu \mathrm{Re}},\ Gr_h=\frac{g\beta_T(\overline{T}-\overline{T}_\infty)\zeta}{U_0^2},\ Gr_m=\frac{g\beta_C(\overline{C}-\overline{C}_\infty)\zeta}{U_0^2},\ \eta=\xi\sqrt{\frac{U}{\nu\zeta}},\\&Du=\frac{D_m K_T(\overline{C}-\overline{C}_\infty)}{\nu C_S C_P(\overline{T}-\overline{T}_\infty)},\ S_r=\frac{D_m K_T(\overline{T}-\overline{T}_\infty)}{\nu C_S C_P(\overline{C}-\overline{C}_\infty)},\ S=\frac{a}{b}<1,\ \nu_\infty=\frac{\mu_\infty}{\rho},\ K=\frac{\nu\zeta}{U_0 K_P},\\&Pr=\frac{\mu C_P}{\lambda},\ Sc=\frac{\nu_\infty}{D_m},\ Re=\frac{U_0\zeta}{\nu},\ Q=\frac{Q_0\zeta}{U_0},\ T(\eta)=\frac{\overline{T}-\overline{T}_\infty}{\overline{T}_w-\overline{T}_\infty},\ C(\eta)=\frac{\overline{C}-\overline{C}_\infty}{\overline{C}_w-\overline{C}_\infty},\\&\psi=\sqrt{\nu\zeta U_0}f(\eta),\ R_a=\frac{32\sigma T_\infty^3}{3\overline{a}\lambda},\ Ec=\frac{U_0^2}{\lambda(\overline{T}_w-\overline{T}_\infty)},\ T_r=\frac{\overline{T}-\overline{T}_r}{\overline{T}_w-\overline{T}_\infty},\ T_C=\frac{\overline{T}-\overline{T}_C}{\overline{T}_w-\overline{T}_\infty}\end{aligned}\right\} \tag{10}$$

Using the transformations (7) to (10), equations (2) to (4) reduced to

$$\frac{T_r}{\left(T-T_r\right)^2}f''T'-\frac{T_r}{T-T_r}f'''-(H_a+K)f'+Gr_h T+Gr_m C+\frac{1}{2}f f''=0, \tag{11}$$

$$-\frac{T_C}{T-T_C}T''+\frac{T_C}{\left(T-T_C\right)^2}\left(T'\right)^2+Pr\,Du\,C''+Pr\,Q\,T+\frac{1}{2}Pr\,f\,T'+Ec\left(f''\right)^2+R_a T''=0, \tag{12}$$

$$C''+\frac{1}{2}Sc\,f\,C'+S_r\,Sc\,T''=0, \tag{13}$$

where primes denote differentiation with respect to η. With boundary conditions,

$$\left.\begin{aligned}&f(0)=0,\ f'(0)=1,\ T(0)=1-S,\ C(0)=1,\\&f'(\eta)\to 0,\ T(\eta)\to 0,\ C(\eta)\to 0 \text{ as } \eta\to\infty\end{aligned}\right\} \tag{14}$$

3. Calculations of physical parameters at $\eta=0$

The coefficient of skin friction (C_f) physically means that shear stress at the wall $\eta=0$ and is defined as

Table 1. Variation of magnetic body force (H_a) on C_f, Nu and Sh.

H_a	C_f		Nu		Sh	
	Present	Subhakar *et al.* [23]	Present	Subhakar *et al.* [23]	Present	Subhakar *et al.* [23]
0.0	0.15209	0.15210	0.160241	0.161103	0.231075	0.231105
0.2	0.61321	0.61341	0.210571	0.211057	0.201632	0.201627
0.4	1.05716	1.05720	0.161210	0.161221	0.176150	0.176161
0.6	1.36102	1.36113	0.105131	0.105180	0.136034	0.136109

Table 2. Variation of Schmidt number (Sc) on C_f, Nu and Sh.

H_a	C_f		Nu		Sh	
	Present	Subhakar *et al.* [23]	Present	Subhakar *et al.* [23]	Present	Subhakar *et al.* [23]
0.24	0.751625	0.751631	0.181207	0.181217	0.243264	0.243261
0.62	0.765314	0.765407	0.159127	0.159131	0.327015	0.327021
0.78	0.790124	0.790129	0.154751	0.154759	0.361068	0.361071

Table 3. Variation of Stratification parameter (S) on C_f, Nu and Sh.

S	C_f		Nu		Sh	
	Present	Subhakar *et al.* [23]	Present	Subhakar *et al.* [23]	Present	Subhakar *et al.* [23]
0.0	0.610671	0.611054	0.350184	0.350210	0.251831	0.251820
0.2	0.561370	0.561410	0.251504	0.251520	0.242940	0.242951
0.4	0.531042	0.531059	0.161073	0.161151	0.241519	0.241610
0.8	0.501873	0.501792	0.102573	0.102492	0.238354	0.238347

$$C_f = \frac{2\tau_w}{\rho \mu_\infty^2}, \quad \tau_w = \mu \frac{\partial \overline{U}}{\partial \eta}\bigg|_{\eta=0},$$

where τ_w is the shear stress at $\eta = 0$. The skin friction at $\eta = 0$ with the use of (10) becomes

$$C_f = \frac{2T_r}{1-T_r} Re^{-1/2} f''(0) \Rightarrow \frac{1}{2} Re^{1/2} C_f = \frac{T_r}{1-T_r} f''(0) \tag{15}$$

In fluid dynamics, Nu is defined as Nu = (convection heat transfer) / (fluid conduction heat transfer) at a boundary in a fluid where convection includes both advection (fluid motion) and diffusion (conduction). Nu is introduced to calculate the transfer of heat between a moving fluid and a solid body. The Nusselt number is calculated by multiplying the temperature gradient $(\partial \overline{T} / \partial \eta)$ and the thermal conductivity (λ). A Nusselt number of value one represents heat transfer by pure conduction. The Nusselt number (Nu) physically gives the temperature gradient from the surface $\eta = 0$ to the fluid and is defined as

$$Nu = \frac{\zeta q_w}{\lambda_\infty \left(\overline{T}_w - \overline{T}_\infty\right)}, \quad q_w = -\lambda \frac{\partial \overline{T}}{\partial \eta}\bigg|_{\eta=0},$$

where q_w is the heat flux. On using (10), Nusselt number at $\eta = 0$ is transformed to

$$Nu = \frac{T_C}{1-T_C} Re^{1/2} T'(0) \Rightarrow Re^{-1/2} Nu = \frac{T_C}{1-T_C} T'(0) \tag{16}$$

The Sherwood number (Sh) physically gives the concentration gradient from the surface $\eta = 0$ to the fluid and is defined as

$$Sh = \frac{\zeta M_w Sc}{\nu_\infty \left(\overline{C}_w - \overline{C}_\infty\right)}, \quad M_w = -D \frac{\partial \overline{C}}{\partial \eta}\bigg|_{\eta=0}$$

where M_w is the mass flux. With the help of (10), the Sherwood number (Sh) reduces to

$$Sh = -Re^{1/2} C'(0) \Rightarrow Re^{-1/2} Sh = -C'(0) \tag{17}$$

4. Validity and Accuracy

A comparative analysis of this investigation and the previous result by Subhakar *et al.* [23] over the physical coefficients C_f, Nu and Sh have illustrated in Table 1, when $Pr = 0.71$, $Sc = 0.24$, $Gr_h = 0.1$, $Gr_m = 0.5$, $S = 0.2$, $Du = 0.1$, $S_r = 0.2$, $Q = 0.2$, $T_r = -6$, $T_C = -6$.

Through these Tables 1 – 3, it is seen that the accuracy of the adopted model is well in deed and so the investigation may carry out for better findings over the impact of viscosity and thermal conductivity on the steady state 2D flow.

4.1. Stability and Convergence

In Table 4, we have examined the stability of the numerical scheme through grid invariance test for the nano-fluid velocity, temperature and nanoparticle concentration. When we reducing the step size (d) as well as increasing the number of elements in the same domain, the stability remains unchanged. This shows that the adopted scheme is workable and so it is stable and convergent.

Table 4. Stability Test for the proposed investigation of velocity, Temperature and Concentration.

	$f'(\eta)$			$T(\eta)$			$C(\eta)$		
				d					
η	**0.01**	**0.001**	**0.0001**	**0.01**	**0.001**	**0.0001**	**0.01**	**0.001**	**0.0001**
0	1.000000	1.000000	1.000000	1.000000	1.000000	1.000000	1.000000	1.000000	1.000000
2	0.513123	0.419063	0.357358	0.328021	0.271272	0.207135	0.371072	0.311085	0.245101
4	0.376033	0.209139	0.210514	0.227086	0.151850	0.107105	0.259417	0.203221	0.131381
6	0.246682	0.119974	0.067595	0.151564	0.052445	0.013844	0.154187	0.103520	0.037324
8	0.094096	0.008781	0.002219	0.041105	0.008411	0.004254	0.007462	0.008050	0.001034
10	0.003076	0.000205	0.000205	0.000512	0.001181	0.000251	0.000691	0.000513	0.000057
12	0.000010	0.000031	0.000010	0.000010	0.000102	0.000037	0.000018	0.000014	0.000004
14	0.000000	0.000000	0.000000	0.00000	0.000000	0.000000	0.000000	0.000000	0.000000

5. Results and Discussion

To analyze the major effects due to viscosity and thermal conductivity on the proposed boundary value problem for thermal radiation (R_a) and Solutal Grashof number (Gr_m), we assumed the default physical parameters, unless otherwise stated: $H_a = 0.1$, $Ec = 0.001$, $Gr_h = 0.1$, $Du = 0.2$, $S_r = 0.3$, $Pr = 0.7$, $Sc = 0.2$, $S = 0.2$, $Re = 0.2$.

In fluid mechanics, viscosity ($T_r > 0$) is defined as the measure of the resistance of a fluid to gradual deformation by shear or tensile stress, which means that viscosity, describes a fluid's resistance to flow. In liquids and gases, viscosity is caused by their molecular makeup. The concept of negative viscosity ($T_r < 0$) asserts that the momentum is transferred from a region of lower velocity toward a flow of higher velocity, increasing the mean wind shear. In general, for any fluids, when the temperature is increased, its density decreases, thus the fluid becomes less viscous. In general when temperature is high, T_r increases in gases and reduces in liquids, and the same will happen for the drag force.

The thermal conductivity is expressed by the well know Fourier's Law of heat conduction which is $q_w = -\lambda(\partial\overline{T} / \partial\eta)$, where q_w is the heat flux, λ is the thermal conductivity, and $(\partial\overline{T} / \partial\eta)$ is the temperature gradient. The negative sign in q_w means that temperature declines in the direction of heat transport and, therefore, $(\partial\overline{T} / \partial\eta)$ is a negative quantity. λ signifies the intrinsic ability of a material to transfer heat or to conduct heat. Heat transfers along a temperature gradient, from high temperature and high molecular energy region to a lower temperature and lower molecular energy region. λ is the heat flows from one part of the body to another body with contact. Basically, λ depends on the $(\partial\overline{T} / \partial\eta)$, the properties of molecules, and the path of heat transfer.

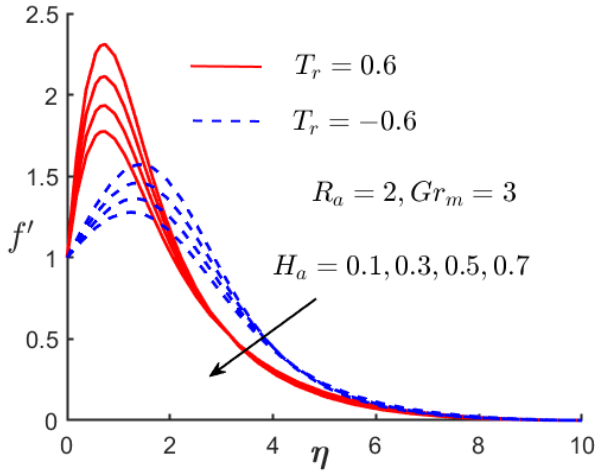

Fig. 2(a). Velocity distribution due to viscosity and magnetic field.

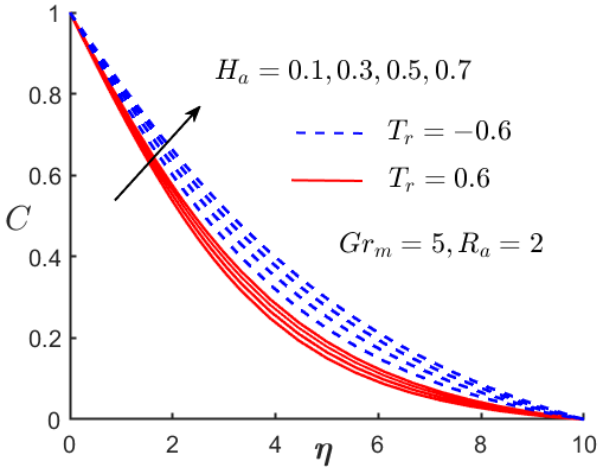

Fig. 2(b). Concentration distribution due to viscosity and magnetic field.

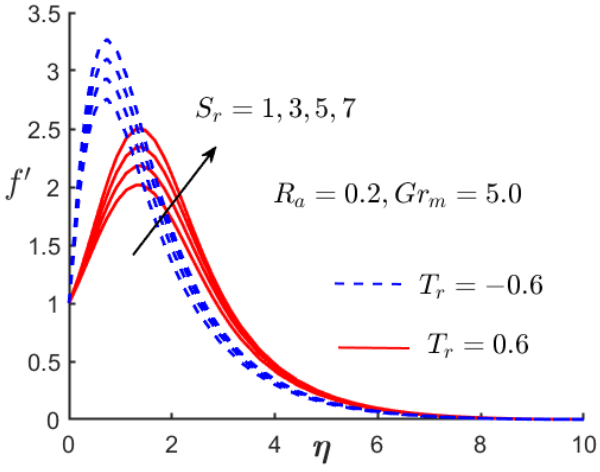

Fig. 3(a). Velocity distribution due to viscosity and Soret.

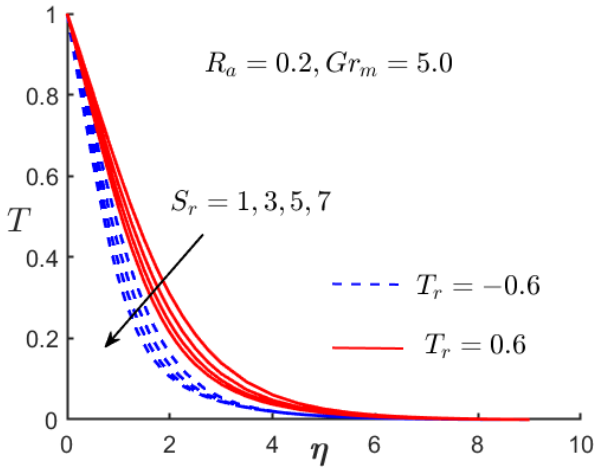

Fig. 3(b). Temperature distribution due to viscosity and Soret.

The variation of viscosity on velocity and concentration for the effect of magnetic drag force has illustrated in Figs. 2(a – b). Julius Hartmann [42] was the initiator to introduce Hartmann number for fluid flows in presence of magnetic field, and is defines as H_a = (electromagnetic force) / (the viscous force). This force is called drag force, and is due to the interaction of electrically conducting fluids with an externally applied magnetic field, which thereafter dragging the magnetic system along the flow direction. The force depends linearly on the mean velocity of the fluid flow. Under this drag force the movement of molecules of the fluid become slow, and it is caused by the Lorentz force (after Hendrik A. Lorentz [43]) which resists the flow motion. Physically it is well known that, MHD drag force always retard the movement of fluid particles and the Concentration equation has a partial involvement with MHD, and so it raises. Here $T_r > 0$ means natural viscosity and $T_r < 0$ is against the viscosity that means no viscosity. Hence the free movement of the fluid particles may exists for $T_r < 0$ and slow movement is occurred for $T_r > 0$ towards $\eta = 0$, however away the surface it is quite reversed. Conversely, the behaviour of viscosity on Concentration plays a significant role, opposite to fluid velocity.

In Fig. 3(a), all the paths of the fluid particles are perfectly elevated near the surface by the influence of S_r and T_r . Soret number (S_r) after the name of C. Ludwig [40, 41] is defined as S_r = (temperature difference) / (concentration difference) and it is also known as thermal diffusion, and under this effect the molecules of mixtures are separated in presence of temperature gradient. Therefore, higher temperature differences and gradient precipitous can be found due to large thermal diffusion and hence higher thermal diffusion enhances the fluid velocity. The Soret effect is available in the lighter molecules of little amount and large heavy molecules under a temperature gradient. This effect is found in the species continuity equation and it is a mass flux due to a temperature gradient. This physical effect is marked in mixtures of moving molecules which responses to the force of a temperature gradient. Here all the curves of velocity have been increased by the Arithmetic Progression of S_r . Conversely, negative viscosity raises the curves of f' and positive viscosity suppresses the curves of f'. The movements of the particles are looking reversed due to the variation of viscosity away the surface $\eta = 0$. The behaviour of T is presented in Fig. 3(b) whose trend is reversed to f' cited in Fig. 3(a). Due to variation of T_r , the thickness of thermal layer of T is enhanced, while heat is transmitted from higher medium to lower medium towards the surface when S_r is upraised.

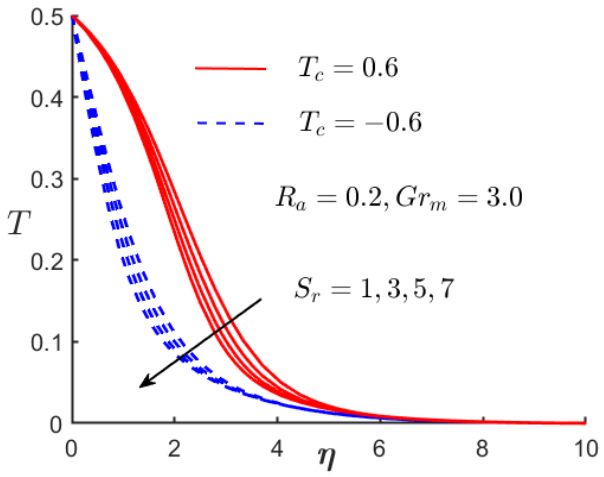

Fig. 4(a). Temperature distribution due to variation of thermal-conductivity and Soret.

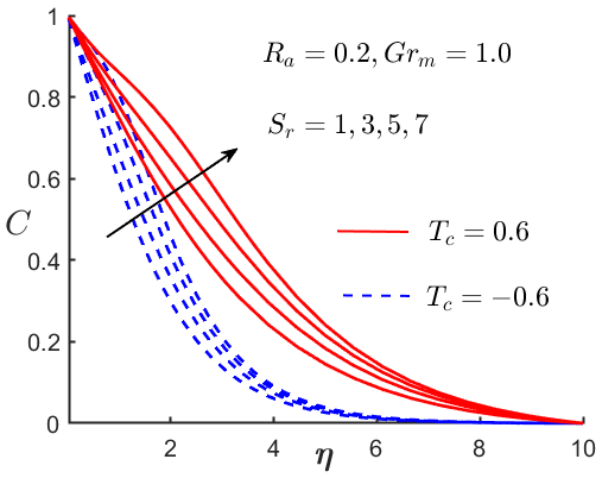

Fig. 4(b). Concentration distribution due to variation of thermal-conductivity and Soret.

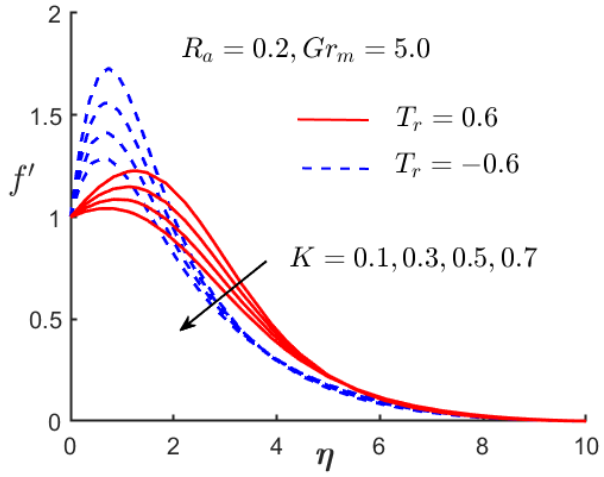

Fig. 5(a). Velocity distribution due to variation of viscosity and Porosity.

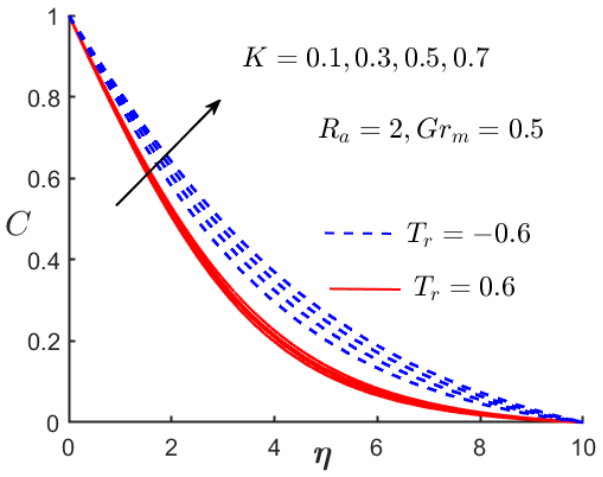

Fig. 5(b). Concentration distribution due to variation of viscosity and Porosity effect.

Figures 4(a – b) indicate the variation of thermal conductivity and Soret effect in temperature (T) and Concentration (C) distributions. The S_r reduces the thickness of thermal layer, while it is increased in Concentration layer. An increase of thermal conductivity of a gas ($Pr = 0.7$), increases the free electrons and lattice vibrations and which leads to increase in gas temperature. Moreover, the species Concentration is partially depending upon thermal conductivity, and so a similar behaviour has occurred like gas temperature. $T_C > 0$ responds the faster rate of heat transfer by the fluid molecules and it increases the energy, while $T_C < 0$ asserts the negative heat transfer which leads to decrease the energy of the fluid molecules. In this study, the fluid is considered as gas ($Pr = 0.7$) which signifies that the thermal conduction has been influenced by the molecules diffusion from higher energy to the lower energy.

The variation of viscosity and Porosity are studied for flow velocity and species Concentration in Figs. 5(a – b). A porous medium is a material containing pores or voids. A porous medium can be defined as a solid, or collection of solid bodies, with sufficient open space in or around the solids to enable a fluid to pass through or around them. Porosity (K) is defined as $K =$ (volume of pores) / (volume of bulk solid bodies) and is usually expressed as a percentage. Porosity = (Volume of Voids / Total Volume) x 100%. Different applications are encountered in geothermal sciences, engineering, biological applications and agriculture. The drag force of porosity retards the motion by the particles of fluid velocity, but the molecules of species is enhanced the Concentration in porous medium. The viscosity retards the motion of the fluid particles near the surface $\eta = 0$, while this trend is opposite towards to the free stream. On the other hand, the molecules of species reduce the width of concentration layer by the variation of viscosity.

At $T_r = -6$, $T_C = -6$, the variation of Ec and R_a over f' and T has been displayed in Figs. 6(a – b) respectively. The Eckert number (Ec) in fluid dynamics was named after Ernst Rudolph Georg Eckert is a dimensionless number and is measured as Ec = (kinetic energy of the flow) / (enthalpy difference). Positive values of Ec correspond to plate cooling, i.e. loss of heat from the plate to the fluid. Also we note that increasing Ec causes an increase in Joule heating as the magnetic field adds energy to the fluid boundary layer due to the work done in dragging the fluid. Due to the variation of dissipative heat, f' declines closer to the surface ($\eta \to \infty$) and enhances away from the surface ($\eta \to \infty$), while T raises for Ec. Thermal radiation, process by which energy, in the form of electromagnetic radiation, is emitted by a heated surface in all directions and travels directly to its point of absorption at the speed of light; thermal radiation does not require an intervening medium to carry it. The Stefan-Boltzmann law of radiation determines the rate of heat transfer by emitted radiation. The thermal radiation arises only in the energy equation in the thermal diffusion term, and via coupling of the temperature field (T) with the buoyancy terms in the momentum equation, the velocity field is indirectly influenced by thermal radiation effects. For $R_a > 1$ thermal radiation is dominant over conduction and vice versa for $R_a < 1$. Higher values of R_a augmented the numerical values of T. However, f' is elevated closer to the surface when R_a is greater, but at $\eta \to \infty$ the higher $R_a = 5.0$ declines the curves of f' and gradually all the paths of the particles moves asymptotically towards the free stream.

The effects of Hartmann drag force (H_a), viscosity (T_r) and thermal conductivity (T_C) over C_f and Nu are exhibited in the following Tables 4 – 5 when: $Pr = 0.7$, $Sc = 0.24$, $Gr_h = 0.1$, $Gr_m = 0.5$, $S = 0.2$, $Du = 0.1$, $S_r = 0.3$, $Q = 0.3$, $T_r = -6$, $T_C = -6$.

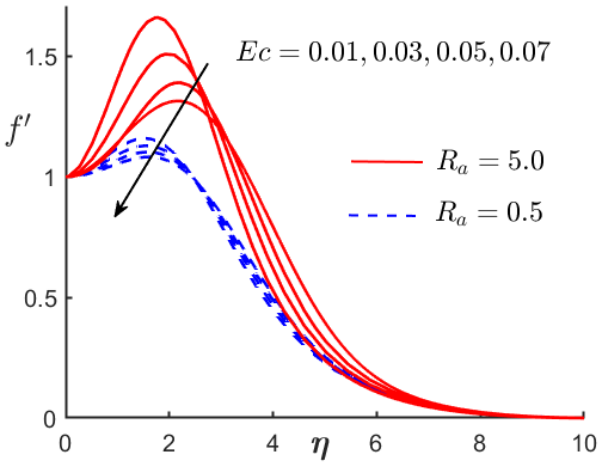

Fig. 6(a). Velocity distribution due to variation of Ec and R_a.

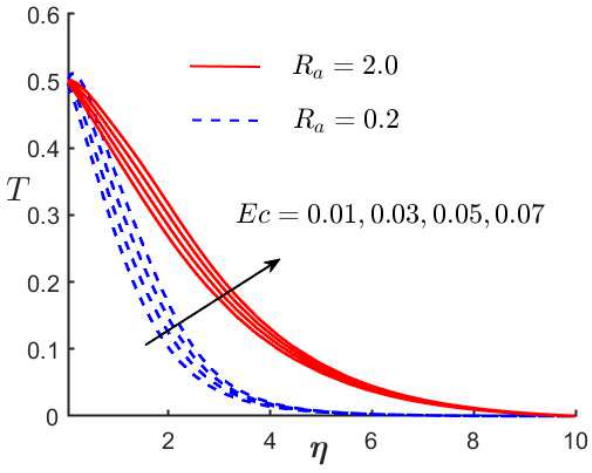

Fig. 6(b). Temperature distribution due to variation of Ec and R_a.

Table 5. Variation of H_a and T_r over C_f and Nu.

H_a	0.0		0.2		0.4	
T_r	C_f	Nu	C_f	Nu	C_f	Nu
-6	0.25192	0.21387	0.75187	0.12790	1.31581	0.10531
-4	0.24087	0.21207	0.71804	0.11539	1.31207	0.10089
-2	0.21309	0.21172	0.64709	0.10318	1.18075	0.08719
2	0.56109	0.21351	1.41995	0.14817	2.14904	0.11715
4	0.46275	0.20647	1.12224	0.13591	1.71504	0.10518
6	0.43715	0.20492	1.05663	0.13418	1.62701	0.09152

Table 6. Variation of H_a and T_C over C_f and Nu .

H_a	0.0		0.2		0.4	
T_C	C_f	Nu	C_f	Nu	C_f	Nu
-6	0.27410	0.21706	0.79103	0.14198	1.18617	0.07519
-4	0.27573	0.21372	0.79210	0.13718	1.18719	0.07354
-2	0.27613	0.19072	0.79317	0.13131	1.18857	0.06638
2	0.28137	0.25417	0.79017	0.17618	1.18358	0.12523
4	0.28149	0.23827	0.79025	0.16917	1.18516	0.12218
6	0.28161	0.23197	0.79041	0.16410	1.18674	0.11087

In Table 5, increasing hydro-magnetic drag force (H_a) leads to incline C_f, while opposite behavior of Nu occurred for H_a. The variation of viscosity (T_r) declines both C_f and Nu. Higher numerical values of C_f and Nu are landed in Table – 5 for the positive viscosity ($T_r > 0$) than the negative viscosity ($T_r < 0$).

For the variation of H_a and T_C in Table – 6, the skin-friction (C_f) raises, while reverse numerical values of Nu emerges over H_a and T_C. Positive thermal conductivity ($T_C > 0$) gives rise the higher values of Nu at $H_a = 0.0, 0.2, 0.4$, in comparison with $T_C < 0$. However, negative thermal conductivity ($T_C < 0$) signifies the maximum values for C_f at $H_a = 0.0, 0.2, 0.4$, and opposite numerical values of C_f are calculated without H_a.

6. Conclusion

In this investigation, we have presented the suitable impact of Viscosity and thermal-conductivity on steady 2D flow along a vertical surface with the drag force of magnetic field and porosity. During calculations, the fluid medium is considered as gas (Air $Pr = 0.7$). Viscosity of fluid always resists the movement of fluid particles and significantly negative viscosity helps to free movement of particles means propel the flow, which is nothing but adding energy to the flow out of nowhere, which is against the law of thermodynamics. When temperature raises, the number of free-electrons and lattice-vibrations gradually increase and so T_C of the metal is likely to rise. In gases, molecular collisions rise with the growth in temperature. Thus, the T_C of a gas upsurges with growth in temperature. As T_C of a specific material is extremely depend on the temperature gradient, the properties of the material, and the path where the heat flows. Due to viscosity, the slow motion has occurred when magnetic drag force is active, while the free movement of particles is seen when porosity is working.

Author Contributions

S. Ahmed contributed the planning of the flow model and Mathematical verifications, while S. Hazarika explored the research methodology section and all figures. All authors discussed the results, reviewed and approved the final version of the manuscript.

Acknowledgements

The authors would like to thank the reviewer's for their valuable comments that improved the manuscript.

Conflict of Interest

The authors declared no potential conflicts of interest with respect to the research, authorship and publication of this article.

Funding

The authors received no financial support for the research, authorship and publication of this article.

Data Availability Statements

The datasets generated and/or analyzed during the current study are available from the corresponding author on reasonable request.

Nomenclature

$\overline{C}$	dimensional concentration [mol/m^3]	Re	Reynolds number
C	dimensionless concentration	Sc	Schmidt number
C_P	specific heat at constant pressure	S_r	Soret number
C_S	concentration susceptibility	$\overline{T}$	dimensional temperature [K]
$\overline{C}_w$	species concentration at the surface [mol/m^3]	T_C	dimensionless thermal conductivity
$\overline{C}_\infty$	species concentration at away from the surface [mol/m^3]	T_m	mean fluid temperature [K]
D_m	mass diffusivity	T_r	dimensionless viscosity
Du	Dufour effect	$\overline{T}_w$	temperature at the surface [K]
Ec	Eckert number	$\overline{T}_\infty$	temperature at away from the surface
f'	dimensionless velocity	U_0	surface velocity
g	acceleration due to gravity	$\overline{U}$	dimensional velocity along ζ -axis [m/s]
Gr_h	thermal Grashof number	$\overline{V}$	dimensional velocity along ξ -axis [m/s]

Gr_m	solutal Grashof number
H_a	Hartmann number
H_0	magnetic field strength
K_T	thermal diffusion ratio
K_P	dimensional porosity parameter
K	dimensionless porosity parameter
Pr	Prandtl number
Q	dimensionless heat generation parameter
Q_0	dimensional parameter of heat generation
q_r	dimensional thermal radiation
R_a	dimensionless thermal radiation parameter
S	stratification parameter
a, b	constants

Greek symbols

β_T	thermal spreading coefficient [K^{-1}]
β_C	concentration spreading coefficient
σ	electrical conductivity of the fluid [Sm^{-1}]
λ	thermal conductivity [W(mK)]
μ	dynamic viscosity [$m^{-1}.s^{-1}$]
μ_∞	dynamic viscosity at $\overline{T}_\infty$ [$m^{-1}.s^{-1}$]
ν_∞	kinematic viscosity at $\overline{T}_\infty$ [$m^{-1}.s^{-1}$]
η	non-dimensional similarity variable
ψ	Steam function
ρ	density of the fluid [kg/m^3]
λ_∞	thermal conductivity at $\overline{T}_\infty$ [W(mK)]

References

[1] Chakrabarti, A., Gupta, A.S., Hydromagnetic flow and heat transfer over a stretching sheet, *Quarterly of Applied Mathematics,* 37, 1979, 73–80.
[2] Sakiadis, B.C., Boundary layer behaviour on continuous solid surface: I. Boundary-layer equations for two-dimensional and axisymmetric flow, *Journal of American Institute of Chemical Engineers*, 7, 1961, 26–28.
[3] Cheesewright, R., Natural Convection from a plate, vertical surface in non-isothermal surroundings, *International Journal of Heat and Mass Transfer*, 10, 1967, 1847-1859.
[4] Helmy, K.A., MHD Unsteady Free Convection flow past a vertical porous plate, *Zeitschrift für Angewandte Mathematik und Mechanik*, 78, 1998, 255-270.
[5] Molla, M.M., Hossain, M.A., Yao, L.S., Radiation effect on mixed convection laminar flow along a vertical wavy surface, *International Journal of Thermal Science*, 43, 2004, 157-163.
[6] Pop, I., Soundalgekar, V.M., Viscous Dissipation effects on Unsteady Free Convective Flow past an infinite vertical porous plate with variable Suction, *International Journal of Heat and Mass Transfer*, 17(1), 1962, 85-92.
[7] Zueco, J., Ahmed, S., López-González, L.M., 2-D Unsteady Free Convective Heat and Mass Transfer Newtonian Hartmann Flow with Thermal Diffusion and Soret Effects: Network Model and Finite Differences, *International Journal of Heat and Mass Transfer*, 110, 2017, 467–475.
[8] Ahmed, S., Zueco, J., López-González, L.M., Numerical and analytical solutions for magneto-hydrodynamic 3D flow through two parallel porous plates, *International Journal of Heat and Mass Transfer,* 108, 2017, 322–331.
[9] Bansal, J.L., *Viscous Fluid Dynamics*, Oxford & IBH Pub. Co., New Delhi, India, 1977.
[10] Herwing, H., Gersten, K., The effect variable properties on Laminar boundary layer Flow, *Warme Stoffubertrag*, 20, 1986, 47–57.
[11] Lai, F.C., Kulacki, F.A., The effect of variable viscosity on convective heat transfer along a vertical surface in a saturated porous medium, *International Journal of Heat and Mass Transfer*, 33, 1990, 1028–31.
[12] Pop, I., Gorla, R.S.R., Rashidi, M.M., The effect of variable viscosity on flow and heat transfer to a continuous moving flat plate, *International Journal of Engineering Science*, 30(1), 1992, 1–6.
[13] Abel, M.S., Khan, S.K., Prasad, K.V., Study of Visco-elastic fluid and heat transfer over a stretching sheet with variable viscosity, *International Journal of Non-linear Mechanics*, 37, 2002, 81–88.
[14] Salem, A.M., Variable viscosity and thermal conductivity effects on MHD flow and heat transfer in viscoelastic fluid over a stretching sheet, *Physics Letter A,* 369(4), 2007, 315–22.
[15] Chiam, T.C., Heat transfer in a fluid with variable thermal conductivity over a linearly stretching sheet, *Acta Mechanica,* 129, 1998, 63–72.
[16] Pantokratoras, A., Further results on the variable viscosity on the flow and heat transfer to a continuous moving flat plate, *International Journal of Engineering Science,* 42, 2004, 1891–96.
[17] Mukhopadhyay, S., Layek, G.C., Effect of thermal radiation and variable fluid viscosity on free convective and heat transfer past a porous stretching surface, *International Journal of Heat and Mass Transfer,* 51, 2008, 2167–78.
[18] Mahanti, N.C., Gaur, P., Effect of varying viscosity and thermal conductivity on steady free convective flow and heat transfer along an isothermal vertical plate in the presence of heat sink, *Journal of Applied Fluid Mechanics*, 2(1), 2009, 23-28.
[19] Sarma, U., Hazarika, G.C., Effect of variable viscosity and thermal conductivity on heat and mass transfer flow along a vertical plate in the presence of magnetic field, *International Journal of Physical Education*, 8(3), 2009, 45–54.
[20] Seddeek, M.A., Salem, A.M., Laminar mixed convection adjacent to vertical continuously stretching sheet with variable viscosity and variable thermal diffusivity, *Heat and Mass Transfer*, 41, 2005, 1048-1055.
[21] Chaim, T.C., Heat transfer in a fluid with variable thermal conductivity over stretching sheet, *Acta Mechanica*, 129, 1998, 63-72.
[22] Chamkha, A.J., Khaled, A.R.A., Similarity solutions for hydromagnetic simultaneous heat and mass transfer by natural convection from an inclined plate with internal heat generation or absorption, *Heat and Mass Transfer,* 37, 2001, 117-123.
[23] Subhakar, M.J., Gangadhar, K., Reddy, N.B., Soret and Dufour effects on MHD convective flow of heat and mass transfer over a moving non-isothermal vertical plate with heat generation/absorption, *Advances in Applied Science Research*, 3(5), 2012, 3165-3184.
[24] Hazarika, G.C., Phukan, B., Ahmed, S., The effect of variable viscosity and thermal conductivity on unsteady free convective flow of a micropolar fluid past a vertical cone, *Journal of Engineering Physics and Thermophysics*, 93, 2020, 184-191.
[25] Schlichting, H., *Boundary Layer Theory*, McGraw-Hill Book Co., New York, 1968.
[26] Sheikholeslami, M., Jafaryar, M., Sheremet, M.A., Shafee, A., Babazadeh, H., Nanomaterial thermal performance within a pipe in presence of turbulator, *Applied Nanoscience*, 10, 2020, 3421–3430.
[27] Wang, G., Yao, Y., Chen, Z., Hu, P., Thermodynamic and optical analyses of a hybrid solar CPV/T system with high solar concentrating uniformity based on spectral beam splitting technology, *Energy*, 166, 2019, 256-266.
[28] Yu, H., Dai, W., Qian, G., Gong, X., Zhou, D., Li, X., Zhou, X., The NOx Degradation Performance of Nano-TiO2 Coating for Asphalt Pavement, *Nanomaterials*, 10(5), 2020, 897.
[29] Guo, C., Hu, M., Li, Z., Duan, F., He, L., Zhang, Z., Du, M., Structural hybridization of bimetallic zeolitic imidazolate framework (ZIF) nanosheets and carbon nanofibers for efficiently sensing ⊠-synuclein oligomers, *Sensors and Actuators B: Chemical*, 309, 2020, 127821.
[30] Liu, C., Huang, X., Wu, Y., Deng, X., Liu, J., Zheng, Z., Hui, D., Review on the research progress of cement-based and geopolymer materials modified by graphene and graphene oxide, *Nanotechnology Reviews*, 9(1), 155-169, 2020.
[31] Yan, H., Xue, X., Chen, W., Wu, X., Dong, J., Liu, Y., Wang, Z., Reversible Na+ insertion/extraction in conductive polypyrrole-decorated NaTi2(PO4)3 nanocomposite with outstanding electrochemical property, *Applied Surface Science*, 530, 2020, 147295.
[32] Luo, X., Hu, H., Pan, Z., Pei, F., Qian, H., Miao, K., Feng, G., Efficient and stable catalysis of hollow Cu9S5 nanospheres in the Fenton-like degradation of organic dyes, *Journal of Hazardous Materials*, 396, 2020, 122735.
[33] He, L., Liu, J., Liu, Y., Cui, B., Hu, B., Wang, M., Du, M., Titanium dioxide encapsulated carbon-nitride nanosheets derived from MXene and melamine-

cyanuric acid composite as a multifunctional electrocatalyst for hydrogen and oxygen evolution reaction and oxygen reduction reaction, *Applied Catalysis B: Environmental*, 248, 2019, 366-379.
[34] Feng, Q., Li, Y., Wang, N., Hao, Y., Chang, J., Wang, Z., Wang, L., A Biomimetic Nanogenerator of Reactive Nitrogen Species Based on Battlefield Transfer Strategy for Enhanced Immunotherapy, *Small*, 16(25), 2020, e2002138.
[35] Liu, Y., Zhang, Q., Xu, M., Yuan, H., Chen, Y., Zhang, J., You, B., Novel and efficient synthesis of Ag-ZnO nanoparticles for the sunlight-induced photocatalytic degradation, *Applied Surface Science*, 476, 2019, 632-640.
[36] Liu, J., Wang, C., Sun, H., Wang, H., Rong, F., He, L., Du, M., CoOx/CoNy nanoparticles encapsulated carbon-nitride nanosheets as an efficiently trifunctional electrocatalyst for overall water splitting and Zn-air battery, *Applied Catalysis B: Environmental*, 279, 2020, 119407.
[37] Ahmed, S., Hazarika, G.C., Gogoi, G., Investigation of variable viscosity and thermal conductivity on MHD mass transfer flow problem over a moving non-isothermal vertical plate, *Journal of Naval Architecture and Marine Engineering*, 17, 2020, 183-197.
[38] Hazarika, S., Ahmed, S., Yao, S.W., Investigation of Cu–water nano-fluid of natural convection hydro-magnetic heat transport in a Darcian porous regime with diffusion-thermo, *Applied Nanoscience*, 2021, https://doi.org/10.1007/s13204-020-01655-w.
[39] Hazarika, S., Ahmed, S., Study of Carbon Nanotubes with Casson Fluid in a Vertical Channel of Porous Media for Hydromagnetic Drag Force and Diffusion-Thermo, *Journal of Scientific Research*, 13(1), 2021, 31–45.
[40] Ludwig, C., *Sitz. ber. Math.-Naturw. Clas. Kais. Akad. Wiss.* 20, 1856, 539.
[41] Soret, C., *Arch. Sci. Phys. Nat.*, 2, 1879, 48.
[42] Hartmann, J., Hg-Dynamics-I, Theory of the laminar flow of an electrically conducting liquid in a homogeneous magnetic field, *Kgl, Danske Videnskab. Selskab Mat-Fys. Medd*, 15(6), 1937, 1-28.
[43] Lorentz, H.A., La Théorie electromagnétique de Maxwell et son application aux corps mouvants, *Archives Néerlandaises des Sciences Exactes et Naturelles*, 25, 1892, 363–552.

ORCID iD

Silpi Hazarika https://orcid.org/0000-0003-1180-1017
Sahin Ahmed https://orcid.org/0000-0001-9606-484x

How to cite this article: Hazarika S., Ahmed S. Theoretical Investigation of Viscosity and Thermal Conductivity of a Gas along a Non-isothermal Vertical Surface in Porous Environment with Dissipative Heat: Numerical Technique, *J. Appl. Comput. Mech.*, 8(4), 2022, 1236–1245. https://doi.org/10.22055/JACM.2021.35353.2638